Reactions of HOCl + HCl + nH$_2$O and HOCl + HBr + nH$_2$O

Andreas F. Voegele, Christofer S. Tautermann, Thomas Loerting,† and Klaus R. Liedl*

Institute of General, Inorganic and Theoretical Chemistry, University of Innsbruck, Innrain 52a, A-6020 Innsbruck, Austria

Received: January 25, 2002; In Final Form: April 15, 2002

We present reaction rates for the conversion of HOCl by HCl and HBr into Cl_2 and BrCl, respectively, supported by $n = 0$, 1, 2, and 3 water molecules. The reaction rates were determined using canonical, variational transition-state theory including tunneling corrections for motion along the reaction coordinate. Whereas the potential energy surface between reactants, transition state, and products was generated with the hybrid density functional theory B3LYP/6-31+G(d), the reaction barrier was determined with the recently developed MPW1K/6-31+G(d,p) hybrid density functional theory, a method that was especially designed to evaluate reaction barriers. Within the used density functional theory framework, the reaction rates of HOCl with HBr are several orders of magnitude higher than the reaction rates with HCl. On ice-like clusters, both types of reactions proceed faster by several orders of magnitude than in the gas phase or when supported by only one or two water molecules. Knowledge of the reaction rates is important in estimating which reaction will occur under stratospheric conditions in the course of ozone depletion.

1. Introduction

Ozone depletion in the stratosphere over Antarctica and Arctica is caused to a great extent by catalytic reactions of ozone with chlorine radicals and to a smaller extent by reactions with bromine radicals.[1−5] Halogen atoms are stored in nearly inert reservoir species ($ClONO_2$, HCl, and HBr) and released into more active forms through several reactions that occur mainly on polar stratospheric clouds (PSC).[6] One of the main reactions is the hydrolysis of $ClONO_2$ that produces HOCl. There are two common ways in which HOCl can react further. First, if HOCl is desorbed from the PSC, it will be quickly photolyzed by sunlight where reactive species such as the HO• and Cl• radicals are formed. Second, in the presence of HCl or HBr, it is very likely that HOCl reacts with one of these molecules.[7,8]

$$HOCl + HCl \rightleftarrows Cl_2 + H_2O \quad (1)$$

$$HOCl + HBr \rightleftarrows BrCl + H_2O \quad (2)$$

Both reactions 1 and 2 are known to occur mainly heterogeneously in the stratosphere whereas the homogeneous gas-phase reactions are considered to be more or less unimportant.[9−11] Reactions 1 and 2 are crucial steps for the final release of reactive halogen species in the stratosphere.

Because of the great importance of both reactions, there are not only experimental but also several theoretical studies on the reaction of HOCl with HCl.[12−15] Apart from studies investigating the reaction, there are also studies on the interactions of HCl[16−21] and HOCl[16,21−24] with water/ice clusters, respectively. Most of the theoretical studies have concentrated on the influence of (a) water molecules on the adsorption behavior of single species,[16−23] (b) water molecules on the reaction barrier,[14,15] and (c) an anion[12] on the reaction barrier. Kroes and Clary[16] determined adsorption energies for HCl and HOCl on ice with trajectory methods whereas Geiger et al.[21] determined the adsorption energies by using water clusters and ab initio methods. An extended study of the HOCl adsorption on model ice was performed by Brown and Doren[23] using a cluster of 26 water molecules. Liu et al. performed ab initio molecular dynamics simulations of the reaction HCl + HOCl on an ice surface using plane waves in their density functional theory approach.[13] In a detailed study, Xu[14] investigated the reaction of HOCl with HCl in water clusters of different sizes with ab initio methods. Xu reports that the reaction barrier is lowered systematically by including "active" water molecules in the reaction. Active in this respect means that the water molecules take part actively in the reaction serving as a proton donor and acceptor in a proton-transfer mechanism and that water molecules do not serve only as spectators. In the course of an uncatalyzed reaction ($n = 0$), the barrier is 55.3 kcal mol^{-1} whereas for the water-catalyzed reactions it decreases to 48.1 kcal mol^{-1} ($n = 1$), 16.1 kcal mol^{-1} ($n = 2$), and 14.4 kcal mol^{-1} ($n = 3$) at the MP2//HF/6-31G(d) level of theory. A proposed mechanism involving four water molecules has a barrier of 45 kcal mol^{-1}, which reflects the fact that a simple increase in the number of active water molecules is not sufficient to obtain an almost barrierless reaction, as would be expected in solution. Xu also showed that inclusion of so-called structural or spectator water molecules lowers the barrier significantly, down to an almost barrierless situation.[14]

To the best of our knowledge, there has been no theoretical study on the reaction of HOCl + HBr, and thus no comparison between the reactions HOCl + HCl and HOCl + HBr has been performed. In this study, we address both reactions and make a comparison between them using ab initio methods and variational transition-state theory to calculate reaction rates. Calculating reaction rates makes it possible to quantify the reaction rate difference between the gas-phase reaction and the heterogeneous reaction on an ice surface (described by water clusters). Finally, we want to evaluate the performance of different ab initio methods for the described reactions.

* Corresponding author. E-mail: Klaus.Liedl@uibk.ac.at. Tel.: +43-512-507-5164. Fax: +43-512-507-5144

† Present address: Department of Earth, Atmosphere and Planetary Sciences, Massachusetts Institute of Technology, 77 Massachusetts Avenue, Cambridge, Massachusetts 02139-4307.

10.1021/jp0255583 CCC: $22.00
Published on Web 07/26/2002

2. Methods

2.1. Stationary Points. Stationary points were calculated with two different hybrid density functional theory (DFT) methods, namely, B3LYP/6-31+G(d)[25] and MPW1K/6-31+G(d,p).[26] The nature of these stationary points was confirmed by vibrational analysis. For optimization of the saddle point, we employed the three-structure quadratic synchronous transit-guided approach.[27] Because classical DFT and hybrid DFT methods such as B3LYP tend to underestimate reaction barriers,[26,28−30] we employed the recently developed modified Perdew−Wang 1-parameter model for kinetics (MPW1K) hybrid DFT method of Lynch et al.[26] This method was especially designed for the purpose of determining reaction barriers to be applied to reaction rate constant calculations. MPW1K uses a modified Perdew−Wang gradient-corrected correlation functional[26,31−33] and a 42.8% Hartree−Fock exchange. Within a test set of 40 reaction barriers, MPW1K has mean signed, mean unsigned, and root-mean-square errors of −1.2, 1.6, and 2.1 kcal mol^{-1}, respectively, compared to experiment; therefore, this method is significantly better than the more commonly used BH&HLYP, B3LYP, or MPW1PW91[26,34] methods. However, this test set contains mainly hydrocarbon reactions, only four reactions containing Cl species, and no reactions containing Br species. Because MPW1K has not been optimized to one of the title reactions or at least a very similar reaction, we have to consider the fact that the results might deviate from the experimental results by a few kcal mol^{-1}. MPW1K was optimized using the 6-31+G(d,p) basis set; therefore, the same basis set will be used throughout this study.

Additionally, we employed high-level methods to evaluate more accurate reaction barriers. To describe reaction rates by transition-state theory, it is necessary to evaluate precise reaction barriers because of the exponential relationship between the reaction barrier and reaction rate. Therefore, we used Gaussian-2 theory [G2(MP2)][35,36] and Gaussian-3 theory [G3 and G3(MP2)][37,38] for some of the systems studied. Both the Gaussian-2 and Gaussian-3 theories employ quadratic configuration interaction with single, double, and perturbational triple excitations [QCISD(T)] but with different basis sets. G2(MP2) uses the triple-ζ 6-311G(d,p) basis set, which is remarkably larger than the double-ζ 6-31G(d) basis set used in G3(MP2). The quality of the QCISD(T) calculation in G3 and G3(MP2) is significantly lower than in G2(MP2). Deficiencies in the basis set are accounted for in both G2 and G3 theory with a basis set extrapolation method employing MP2 and MP4, respectively, which is explained in detail in the original work by Pople and co-workers.[35−38] Briefly, in G2(MP2), one adds the difference between MP2/6-311+G(3df,2p) and MP2/6-311G(d,p) to the QCISD(T)/6-311G(d,p) calculation and gets a good approximation for QCISD(T)/6-311+G(3df,2p). G3(MP2) uses the difference between the energy calculations on the MP2/G3MP2large and MP2(full)/6-31G(d) levels of theory (the G3MP2large basis set is a modified 6-311+G(3df,2p) basis set; for details, see Curtiss et al.[37,38]). In a given test set (G2/97), G3(MP2) performs slightly better than G2(MP2) and is computationally less expensive.[38] We wanted to compare the methods to calculate reaction barriers and reaction energies. As another high-level method, we used coupled cluster theory with single, double, and perturbational triple excitations [CCSD(T)/aug-cc-pVDZ][39] on the geometries we obtained at the MP2/aug-cc-pVDZ[40,41] level of theory [CCSD(T)/aug-cc-pVDZ//MP2/aug-cc-pVDZ]. To test for an appropriate choice of the HF reference wave function, the performance of CCSD(T)/aug-cc-pVDZ was tested by the $\mathcal{T}_1$ diagnostic.[42]

2.2. Reaction Path. By starting from the transition state, the reaction path was created as the steepest descent path in mass-scaled coordinates where the scaling mass of 1 amu was used. To create this so-called minimum-energy path (MEP) or intrinsic reaction coordinate (IRC), the Page−McIver local quadratic approximation algorithm[43] and B3LYP/6-31+G(d) were used at a step size of 0.050 Bohr (0.026 Å). Distances on the potential energy surface from the transition state are denoted s, where s is positive on the product side and negative on the educt side. Every third point along the potential energy surface's second derivatives and partition functions was calculated. The path was calculated on both sides of the transition state until stable minimum structures were reached (i.e., when the gradient had almost vanished). B3LYP in general describes geometries and energy hypersurfaces well but underestimates the height of reaction barriers (as mentioned previously). Therefore, we interpolated the B3LYP/6-31+G(d) hypersurface to the energy values of the stationary points determined at the MPW1K/6-31+G(d,p) level of theory. Calculating the reaction path and thus the reaction rates on the basis of two different levels of theory is termed dual-level direct dynamics, and the interpolation procedure is called variational transition-state theory with interpolated corrections. The shorthand notation for this procedure is MPW1K/6-31+G(d,p)///B3LYP/6-31+G(d), and the interpolation procedure is based on a logarithmic procedure.[44]

2.3. Reaction Rates and Quantum Mechanical Tunneling. Reaction rates were obtained using transition-state theory (TST)[45] as implemented in Polyrate, version 8.5.1.[46,47] Theoretical details and equations can be found elsewhere;[45,48−54] here we give just a short description of some of the details. A variational approach for TST with a canonical ensemble was used to obtain a rate constant k^{CVT} (CVT = canonical variational TST) that was minimized with respect to barrier crossings. When all bound degrees of freedom are described quantum mechanically, motion along the reaction coordinate cannot be treated quantum mechanically. Therefore, quantum mechanical effects (mainly tunneling effects) along the reaction coordinate are well approximated by semiclassical methods to evaluate transmission probabilities. Inclusion of the quantum mechanical effects on the reaction rate constant is carried out by multiplying the rate constant k^{CVT} by a ground-state transmission coefficient κ. The transmission coefficient is evaluated by different methods that consider that in the course of the reaction the system tunnels along shorter paths that are more demanding in terms of energy. The methods we consider are the crude Wigner tunneling correction, the small curvature tunneling (SCT) approach, and the large curvature tunneling (LCT) approach. The Wigner correction, which was developed in 1932,[55] is based only on the imaginary frequency determined at the transition state and does not include information about the reaction path. SCT is considered by means of the centrifugal dominant small-curvature semiclassical adiabatic ground-state tunneling method according to the concept of Marcus and Coltrin.[56−58] The LCT correction assumes that tunneling occurs through a series of straight line connections between the educt and the product valley. Polyrate employs the large curvature ground-state approximation version 4 (LCG4)[59] for LCT. Depending on the curvature of the reaction path and the temperature, either SCT or LCT becomes predominant; thus, one uses the maximum of these methods to evaluate the tunneling corrections and multiplies it by k^{CVT}. This approach is termed microcanonical optimized multidimensional tunneling (μOMT).

TABLE 1: Selected Reaction Barriers for the Reactions HOCl + HCl and HOCl + HBr Catalyzed by *n* Water Molecules at Different Levels of Theory[a]

	reaction barrier (kcal mol^{-1})				
HOCl + HCl	MP2	CC	G2(MP2)	G3(MP2)	G3
$n = 0$	51.9	44.5 (0.075)	35.3	35.2	64.1
$n = 1$(a)	54.3	47.3 (0.059)	62.1	50.5	
$n = 2$			13.6	12.6	
HOCl + HBr					
$n = 0$	44.1	32.6 (0.079)	48.0		
$n = 1$(a)	46.1				

[a] CC is our shorthand notation for CCSD(T)/aug-cc-pVDZ//MP2/aug-cc-pVDZ, and MP2 stands for MP2/aug-cc-pVDZ. Numbers in parentheses beside the coupled-cluster values are the $\mathcal{T}_1$ values determined for the transition state. Using the aug-cc-pVTZ instead of the DZ basis set did not improve $\mathcal{T}_1$ significantly. Note that we did not calculate all systems at the different levels of theory because of the unsuccessful description of the multideterminant character, as mentioned in the text.

TABLE 2: Reaction Barriers for the Reactions HOCl + HCl and HOCl + HBr Catalyzed by *n* Water Molecules at Different Levels of Theory[a]

	reaction barrier (kcal mol^{-1})			
HOCl + HCl	B3LYP/ 6-31+G(d)		MPW1K/ 6-31+G(d,p)	MP2//HF/ 6-31G(d)[14]
$n = 0$	40.7	42.2[b]	54.7	55.3[b]
$n = 1$ (a)	41.7	42.6[b]	54.7	
$n = 1$ (b)	25.7	27.1[b]	33.1	48.3[b]
$n = 2$	6.53	6.63[b]	9.74	16.1[b]
$n = 3$	4.13	4.12[b]	3.28	14.4[b]
HOCl + HBr				
$n = 0$	31.6	33.5[b]	44.4	
$n = 1$	32.6	34.6[b]	44.6	
$n = 2$	0.89	0.57[b]	0.76	
$n = 3$	0.15	−0.36[b]	0.75	

[a] Energies determined at the MP2//HF/6-31G(d) level are taken from Xu.[14] [b] Corrected for zero-point energy (ZPE).

3. Results and Discussion

3.1. Evaluation of the Methods. We determined most of the reaction barriers for the title reactions at several levels of theory (Table 1 and Table 2 give a brief summary). Unfortunately, there are large differences between most of the methods. G2(MP2), G3(MP2), and G3 differ by up to almost 30 kcal mol^{-1}, clearly indicating that these methods fail to reproduce reaction barriers for the described systems within chemical accuracy. We used the $\mathcal{T}_1$ diagnostic on the coupled-cluster [CCSD(T)/aug-cc-pVDZ//MP2/aug-pVDZ] calculations and evaluated $\mathcal{T}_1$ values for transition states that were clearly larger than 0.04 and sometimes as large as 0.08.[42] $\mathcal{T}_1$ values of that size indicate that the reference wave function does not describe the system satisfactorily and that a multideterminant approach is needed. Because both the coupled-cluster and the Gaussian approaches are based on single-determinant HF wave functions, they suffer from the same error. Therefore, accurate multideterminant methods should be employed, which, considering the number of different reactions studied, would be too time-consuming.[34] We did not evaluate all of the reaction barriers at the higher levels because these calculations would also be too time-consuming, and results of high quality cannot be expected for the larger clusters.

We investigated the change in atom−atom distances between the Cl atom of HOCl, the Cl atom of HCl, and the Br atom of HBr between the reactant and transition states at different levels of theory (see Table 4). A slight trend of an increasing barrier with an increasing change in atom−atom distances could be observed both within a given set of reactions (i.e., rows of Table 4) and within a given method (i.e., columns of Table 4). This trend holds, at least generally, between the B3LYP and MPW1K results, mostly between the DFT and G2(MP2) results, but not with MP2. Thus, the barrier height is very sensitive to the geometry of the studied reactions, so a bad choice of geometry within a given reaction yields bad results for the barrier height.

TABLE 3: Reaction Energies for the Reactions HOCl + HCl and HOCl + HBr Catalyzed by *n* Water Molecules at Different Levels of Theory[a]

	reaction energy (kcal mol^{-1})			
HOCl + HCl	B3LYP/ 6-31+G(d)		MPW1K/ 6-31+G(d,p)	MP2//HF/ 6-31G(d)[14]
$n = 0$	−12.3	−10.8[b]	−12.7	−7.9[b]
$n = 1$ (a)	−8.74	−7.34[b]	−8.92	
$n = 1$ (b)	−17.8	−15.2[b]	−17.8	−9.8[b]
$n = 2$	−16.6	−14.8[b]	−15.5	−12.7[b]
$n = 3$	−15.4	−13.3[b]	−15.6	−16.2[b]
HOCl + HBr				
$n = 0$	−26.0	−24.1[b]	−27.3	
$n = 1$	−30.0	−27.6[b]	−30.6	
$n = 2$	−27.5	−25.3[b]	−28.6	
$n = 3$	−25.3	−24.2[b]	−25.0	

[a] Energies determined at the MP2//HF/6-31G(d) level are taken from Xu.[14] [b] Corrected for zero-point energy (ZPE).

TABLE 4: Change of Cl−Cl and Cl−Br Distance, Respectively, between the Reactant and Transition State Determined at Different Levels of Theory[a]

	Δbond length Cl−Cl/Br (Å)			
HOCl + HCl	B3LYP	MPW1K	MP2	G2(MP2)
$n = 0$	−1.447 (40.7)	−1.580 (54.7)	−1.305 (51.9)	−1.353 (35.3)
$n = 1$ (a)	−1.519 (41.7)	−1.703 (54.7)	−1.277 (54.3)	−1.294 (62.1)
$n = 1$ (b)	−0.717 (25.7)	−0.902 (33.1)		
$n = 2$	−0.660 (6.51)	−0.900 (9.74)		−0.791 (13.6)
$n = 3$	−0.455 (4.10)	−0.303 (3.28)		
HOCl + HBr				
$n = 0$	−1.342 (31.6)	−1.530 (44.4)	−1.209 (44.1)	−1.235 (48.0)
$n = 1$ (a)	−1.017 (32.6)	−1.372 (44.6)	−1.163 (46.1)	
$n = 2$	−0.225 (0.86)	−0.208 (0.76)		
$n = 3$	−0.063 (0.15)	−0.010 (0.75)		

[a] Within each row, the barrier decreases with decreasing Cl−Cl/Br distance.

Because B3LYP underestimates reaction barriers, we used the MPW1K/6-31+G(d,p) barriers that are larger than the B3LYP barriers for most cases (except for HCl and $n = 3$ and HBr and $n = 2$, 3). The MPW1K method was optimized by Lynch et al.[30,34] to predict reaction barriers for kinetic purposes. The values determined with MPW1K were chosen because coupled-cluster and Gaussian methods failed to predict the reaction barriers and are so computationally expensive that all of the systems could not be studied. Additionally, the MPW1K results are very encouraging because they are in much better agreement with the MP2/aug-cc-pVDZ values than with values from other approaches. Possibly, the perturbational and the MPW1K approaches are better choices for this system than the other methods that actually seem plausible because both methods use a different approach than the other post Hartree−Fock methods we used.[60,61]

Reaction barriers are crucial for predicting kinetic properties; therefore, one has to be aware that within the accuracy of MPW1K the error limit is a few kcal mol^{-1}. Considering a

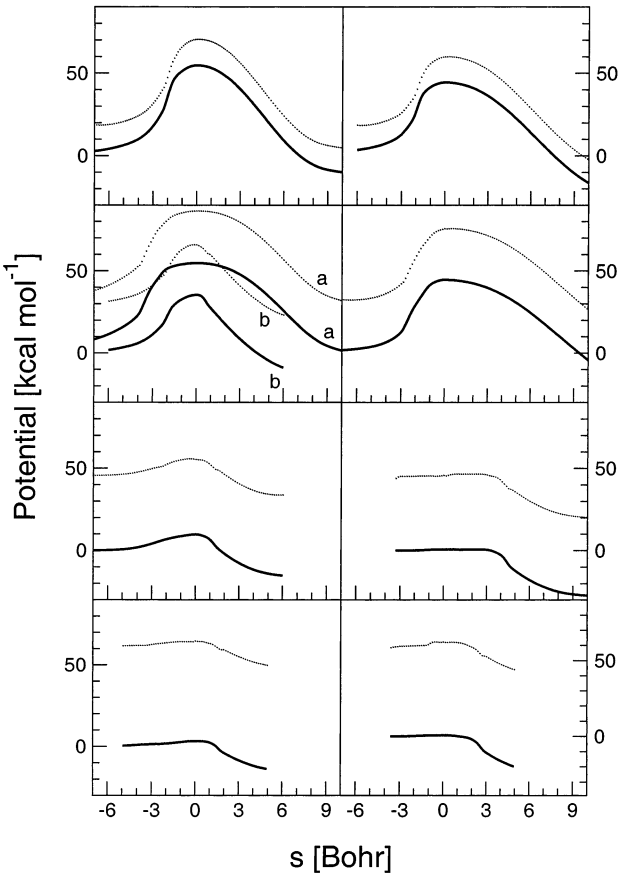

Figure 1. Classical potential energy curve (or minimum-energy path; —) and vibrationally adiabatic ground-state potential energy curve (· · ·) as a function of the reaction coordinate *s* calculated at the B3LYP/6-31+G(d) level of theory interpolated to MPW1K/6-31+G(d,p) energies. Left: HOCl + HCl + nH$_2$O starting from n = 0 (top) to n = 3 (bottom); right: HOCl + HBr + nH$_2$O.

deviation of only between 1 and 2 kcal mol^{-1}, we have to assume that the error in terms of reaction rates is about 1 to 2 orders of magnitude between 200 and 300 K. The reaction rates determined in this study will therefore provide primarily a qualitative picture whereas quantitative properties should be considered to bear an error of a few orders of magnitude. Because our goals are to estimate which of the two reactions is faster and to approximate the difference between the gas-phase and the surface-catalyzed reactions, our results will give a very good picture of which reaction will happen under different conditions.

3.2. Stationary Points and Reaction Mechanisms. 3.2.1. HOCl + HCl. We determined stationary points for the reaction of HOCl + HCl with n = 0, 1, 2, and 3 water molecules (see Figure 2). The structure of the pure HOCl·HCl complex, representing the gas-phase reaction, is characterized by a hydrogen bond, where HCl serves as a proton donor and HOCl, as a proton acceptor. In the course of the reaction, HCl protonizes HOCl and forms a H_2OCl^+·Cl^- -like complex at the transition state that in the following step forms the products Cl_2 and H_2O. The reaction barrier is 54.7 kcal mol^{-1} at the MPW1K/6-31+G(d,p) level of theory, which is in excellent agreement with 55.3 kcal mol^{-1} (with zero-point energy, ZPE) as reported by Xu[14] (barriers and reaction energies are summed up in Tables 1, 2, and 3), yet the geometries of the reactant complex determined in this study differ from the ones determined previously.[14,13] Whereas Liu et al.[13] report a van der Waals complex where the two chlorine atoms are closest, Xu[14] reports a complex where the O−Cl bond is parallel to the H−Cl bond. Zhou and Liu[15] report a complex that is more similar to the one determined in this study, where a hydrogen bond is formed between the oxygen atom and H−Cl. (Geometrical details and a comparison with previous studies are given as Supporting Information).

3.2.2. HOCl + HCl + 1H$_2$O. We found two different local minimum structures for the HOCl·HCl·H$_2$O complex that we termed (a) and (b) (see Figure 2). Complex (a) is the lower-lying minimum compared to (b), with an energy difference of 5.0 kcal mol^{-1}. At 200 K, the ratio of complex (a) to (b) is approximately 10^5. The reaction barriers for the two processes are 54.7 (a) and 33.1 (b) kcal mol^{-1}, respectively. Assuming that both complexes are present, reaction channel (b) would be faster by about 15 to 20 orders of magnitude in the temperature range from 200 to 300 K. The reaction complex determined by Xu[14] resembles our (b) mechanism but is still slightly different. The barrier is higher than in channel (b), and the reaction energy is lower (see Tables 2 and 3) (the geometries are compared in Supporting Information).

In both channel (a) and channel (b), the water molecule acts as a proton shuttle that is responsible for so-called water-mediated proton transfer. Because the barrier of channel (a) is as high as the reaction without an additional water molecule, this mechanism will play no role in the gas phase because it is more likely that a complex of two molecules rather than a complex of three molecules will form.

3.2.3. HOCl + HCl + 2H$_2$O. In the course of the reaction HOCl + HCl with two catalytic water molecules, we can also observe a proton-shuttle mechanism. Both water molecules are directly involved in the reaction. HCl protonates a neighboring water molecule, and this molecule in turn transfers one of its own protons to the second water molecule, which donates one of its protons to HOCl. Finally, this results in a net separation of Cl^- and H_2OCl^+ at the transition state that is similar to that in the uncatalyzed reaction. The catalytic effect of the two water molecules is enormous because the barrier is lowered from 54.7 to 9.7 kcal mol^{-1}. Xu[14] found barriers that were approximately 9.5 and 6.4 kcal mol^{-1} higher than the barriers we found even though the structures are very similar.

3.2.4. HOCl + HCl + 3H$_2$O. Finally, we investigated a mechanism for the reaction of HOCl with HCl involving three water molecules. As shown in Figure 2, the reaction mechanism is very similar to the mechanism occurring on a hexagonal ice surface (see Figure 3). By also taking into account the fact that this reaction is almost barrierless (3.3 kcal mol^{-1}), we can assume that this reaction is representative of the surface reaction on ice. Even though on a real ice surface there would be more water molecules surrounding the reaction complex, we think from a mechanistic point of view that the reaction is described sufficiently. As demonstrated by Xu,[63] the mechanisms found so far involving more than three active water molecules do not occur. Other water molecules only stabilize the complex but do not participate during the reaction. The reaction takes place on a surface; therefore, solvation effects influence the water molecules involved in the reaction. Yet, HOCl and HCl, which are located at the surface,[62] are not influenced very much by the solvation effect of other water molecules.

The mechanism for the reaction involving three water molecules proceeds similarly to the above-mentioned mechanisms where the HCl proton is transferred to the first water molecule, which shuttles one of its own protons to the next water molecule and so forth. Even though the bond length of HCl in the clusters of different size increases with the number of water

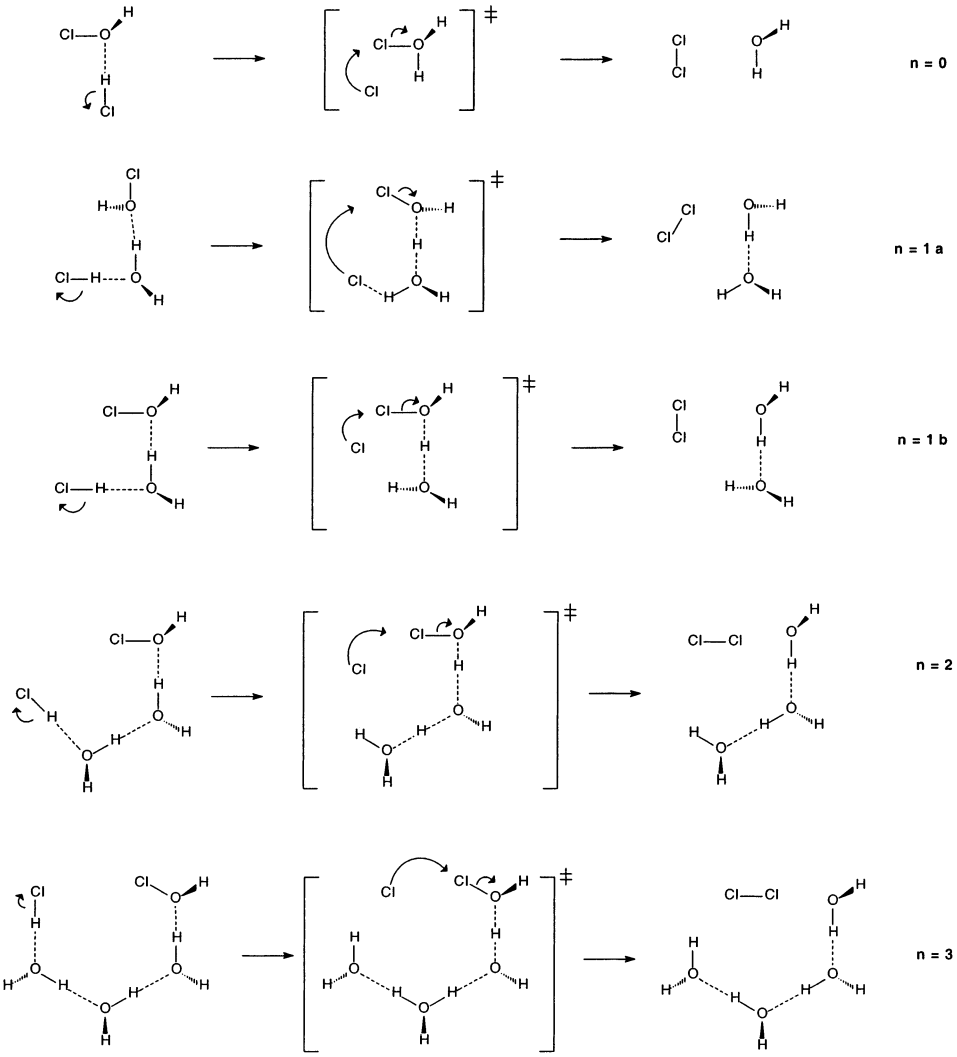

Figure 2. Qualitative representation of the stationary points of the reaction HOCl + HCl supported by $n = 0$, 1, 2, and 3 water molecules. The reactions HOCl + HBr with $n = 0$, 1, 2, and 3 water molecules are analogous except for mechanism (1b), which could not be found for HBr because of the nonconvergence of the transition state.

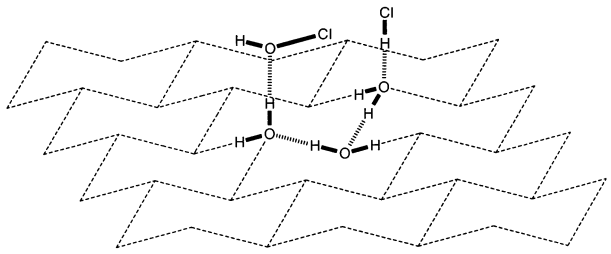

Figure 3. Schematic representation of the reaction complex of HOCl and HCl on a hexagonal ice surface. HCl adsorbs perpendicularly on the ice surface with its hydrogen bond oriented toward a surface oxygen atom. HOCl adsorbs on the ice surface forming a hydrogen bridge between the oxygen atom and a dangling hydrogen of the ice surface. This is the most likely complex on a hexagonal ice surface. The formed complex of HOCl·HCl·ice is almost identical to the mechanism shown in Figure 2 for the mechanism with three water molecules.

molecules involved, we find no Cl^- ion in the reactant state. This is in agreement with the study of Xu,[14] which also reported no dissociation of HCl in clusters of that size. Similar to the $n = 2$ case, the reaction barrier reported by Xu is much higher (10 kcal mol^{-1}) than our barrier even though the geometries are not significantly different (see Supporting Information). The barrier reported by Zhou and Liu[15] is higher than ours, but because they employed a different model for the ice catalyzation, the different result is not surprising.

3.2.5. HOCl + HBr + *n*H_2O. Qualitatively, the picture for HOCl + HBr is almost the same as for the reactions involving HCl. All mechanisms were found to be identical except for mechanism (1b), where the geometry of the transition state did not converge. Because of the different size of the bromine atom compared to the chlorine atom, bond lengths and angles differ a little (see Supporting Information). Quantitatively, the result is different from the HCl cases because the reaction barriers are significantly lower (see Table 2). The mechanisms involving HBr obey a trend of significantly lower reaction barriers than those mechanisms involving HCl. The case for $n = 2$ is almost barrierless, with an energy difference between the educt and transition state of only 0.76 kcal mol^{-1}. A third catalytic water molecule ($n = 3$) does not lower the reaction barrier (0.75 kcal mol^{-1}); therefore, we assume that there are two important mechanisms for this reaction on an ice surface. The ZPE-corrected barrier for $n = 3$ is slightly negative at the B3LYP/6-31+G(d) level, yet when inspecting the potential energy curve (see Figure 1), we find that even though the barrier is negative at the transition state there is a maximum in the potential energy curve off the classical transition state. The maximum of $\Delta G^{\ddagger}$ is temperature-dependent and is crucial to the determination of

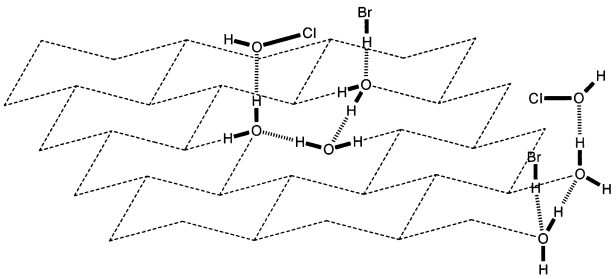

Figure 4. Schematic representation of the reaction complex of HOCl and HBr on a hexagonal ice surface. The mechanism for the case with three active water molecules is identical to the mechanism for HOCl + HCl (see Figure 3). Additionally, a mechanism with two active water molecules might occur, which is shown schematically in the lower right corner. This mechanism is likely to be important for conditions with a high surface coverage with different molecules.

the reaction rate. We found, however, that $\Delta G^{\ddagger}$ at the generalized transition state[49] is positive for any reaction at any temperature and that $\Delta G^{\ddagger}$ is $>RT$ (even though only by 300 cal mol^{-1} for $n = 3$ and $T = 100$ K, thus the VTST approach is still applicable although the result should be used with care). When following the MEP from the transition state, we found no stable intermediates in any of the reactions even though the gradient of the reaction is very small. In both the HCl and HBr reactions, the protons are transferred asynchronously but concertedly.

From the mechanistic point of view, the reactions with $n = 2$ and 3 might occur on hexagonal ice (see Figure 2). In Figure 4, we show schematically how the reactions of HOCl with HBr might occur on an ice surface.

3.3. Reaction Rates and Quantum Mechanical Tunneling. Previous studies on the HOCl + HCl system have described only reaction barriers but not reaction rates. However, the barrier between two reactions is not sufficient for the estimation of differences in reaction rates even if we are interested only in a qualitative and not a quantitative picture. An accurate calculation of rate constants for reactions involving hydrogen atom transfer requires a quantum mechanical treatment of the motion along the reaction coordinate. This in turn requires more knowledge of the potential energy surface than just the barrier height. It turns out that tunneling can increase the reaction rate by many orders of magnitude[64−67] if there is at least one proton transfer involved. Therefore, we determined the tunneling contributions on the reaction rates for the described reactions.

Figure 5 shows all reaction rates in the series HOCl + HCl/HBr supported by different numbers of water molecules. What we can observe is that the reactions involving HBr are in general much faster than the reactions involving HCl. In Figure 5B, the mechanism for HOCl + HBr + H_2O corresponds to the same mechanism as for HOCl + HCl + H_2O (a), but we were unable to determine the mechanism corresponding to HOCl + HCl + H_2O (b). Figure 5D represents the cases for the reactions with three water molecules, which are representative of an ice surface. Because both reactions are almost barrierless, the temperature dependence is small—the HBr reaction is almost independent of temperature changes, and the HCl reaction changes only by a factor of 10 in the temperature range 190 to 300 K. At 190 K, we observed reaction rates of 1×10^8 s^{-1} and 4×10^{11} s^{-1} for HOCl + HCl and HOCl + HBr ($n = 3$), respectively. Therefore, the reaction-rate difference between the two reactions is approximately 4000.

Table 5 summarizes the transmission coefficients at 190 K. Mostly, the small-curvature tunneling approach is predominant over the other forms of tunneling, with some exceptions. For the reaction HOCl + 1HCl + 1H_2O (b) and also for the surface-like reaction of HOCl with HCl, LCT clearly predominates over

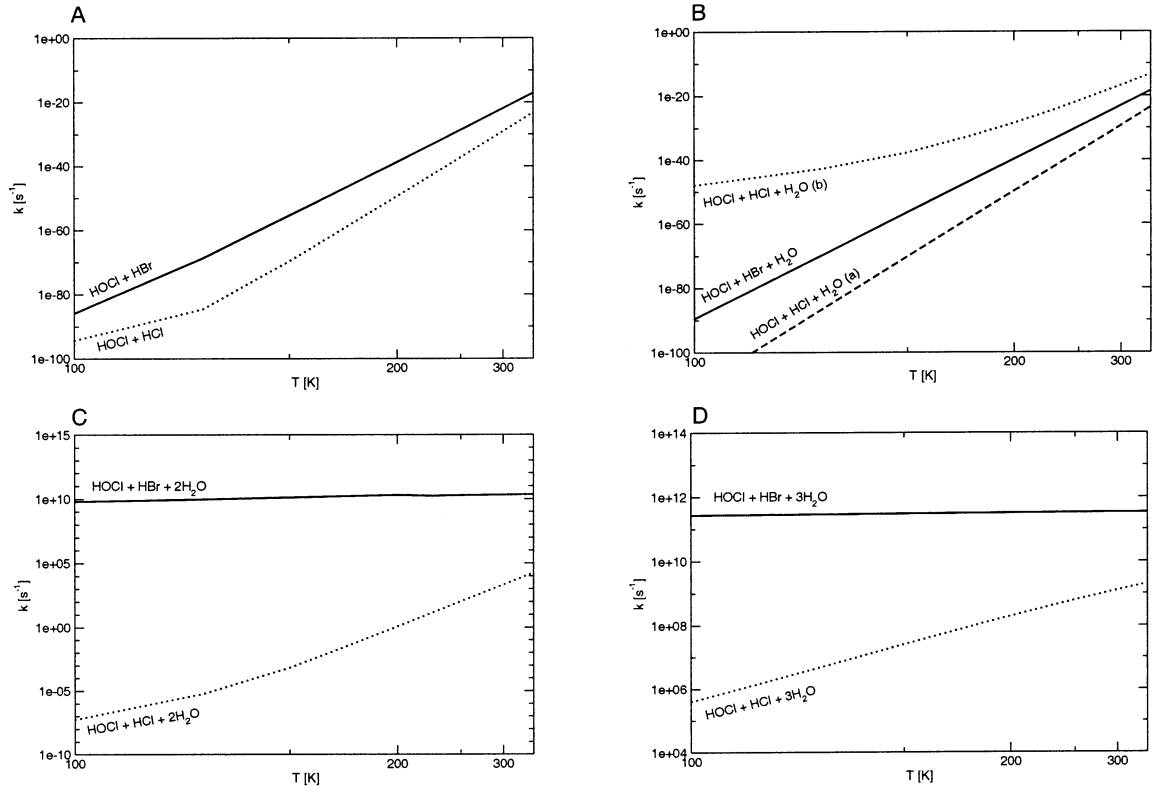

Figure 5. Reaction rates for the reactions of HOCl with HBr. (A), (B), (C), and (D) represent the reactions with $n = 0$, 1, 2, and 3 water molecules, respectively. Shown are reactions with HBr (—) and HCl (• • •) . In (B), reaction channels (a) and (b) are shown for the HCl reaction, as outlined in the text and in Figure 2.

TABLE 5: Transmission Coefficients (Tunneling Corrections) for the HOCl + HCl, HBr Reactions[a]

	transmission coefficient κ at 190 K		
HOCl + HCl	Wigner	LCT	SCT
$n = 0$	1.208	1.701	1.741[a]
$n = 1$ (a)	1.086	1.178	1.182[a]
$n = 1$ (b)	1.482	113.4[a]	23.71
$n = 2$	1.502	1.685	1.723[a]
$n = 3$	1.104	1.882[a]	1.788
HOCl + HBr			
$n = 0$	1.116	1.345	1.385[a]
$n = 1$ (a)	1.044	1.270	1.660[a]
$n = 2$	1.056	1.376	1.579[a]
$n = 3$	1.079	1.142	1.170[a]

[a] Most important form of tunneling (μOMT). $T = 190$ K.

all other tunneling approaches. In most cases, the Wigner correction is not sufficient to describe tunneling. The highest tunneling contribution happens in reactions HOCl + HCl + $1H_2O$ (b) (representative of a gas-phase reaction) and HOCl + HCl + $3H_2O$ (representative of a surface-catalyzed reaction) with κ's of 113 and 1.88, respectively. Thus, we can observe reaction-rate enhancements of 113-fold and 88%, respectively, due to tunneling. The much higher tunneling contribution for 1(b) in comparison to 1(a) might best be explained by inspecting Figure 1. The curvature of the barrier of channel 1(b) is much larger than that for 1(a). A detailed inspection showed that the mechanism of 1(a) works as follows: First, the proton of HOCl rotates by approximately 120° along the Cl−O bond. Next, the two chlorine atoms move approximately 1.5 Å toward each other, thus approximating the transition state. The small curvature and the small tunneling contribution might be best explained by the strong movement of the two chlorine atoms.

Comparing the gas-phase reactions with the surface-catalyzed reactions, we find that the reaction-rate enhancement is 50 orders of magnitude. To illustrate this large difference, we observe that the gas-phase reaction happens within billions of years whereas the surface-catalyzed reaction happens within nanoseconds and femtoseconds.

4. Conclusions

In this study, we have concentrated on the competing reactions of HOCl + HCl and HOCl + HBr either in the gas phase or on water clusters representing a hexagonal ice surface. From the methodological point of view, we saw that the transition state for such types of reactions is not well described with post Hartree−Fock methods such as CCSD(T) or QCISD(T) (as in G2 or G3). Therefore, we used the newly developed MPW1K hybrid-DFT approach by Lynch et al.,[30] who designed this method especially to evaluate reaction barriers. Xu[14] studied the reaction of HOCl + HCl + nH_2O with MP2//HF/6-31G(d) and found higher barriers throughout and shorter bond lengths in the hydrogen-bridged water complexes. When following the minimum-energy paths from the transition states, we found concerted, asynchronous proton transfers for all of the studied systems with no stable intermediate.

We determined reaction rates using transition-state theory including tunneling corrections. Clearly, a trend of increasing reaction rates by including catalytic water molecules in the reaction complex was observed. The uncatalyzed gas-phase reaction is about 50 orders of magnitude slower than the reaction occurring on a cluster representing an ice surface. Tunneling is significant at about 190 K because it accelerates the reaction on the surface up to about 88%. A direct comparison between the HCl and HBr reactions shows that the HBr reactions on the surface tend to be 3 to 4 orders of magnitude faster.

Considering polar stratospheric clouds of type II, we find that the reaction of HOCl with HBr is the more important one as long as the ratio of HBr to HCl is $\geq$1:4000. At present stratospheric HCl and HBr concentrations, the HBr mechanisms are clearly more important. Also, because the HBr reaction can occur via a mechanism involving a smaller reaction cluster, the reaction happens under conditions where not enough water molecules are accessible for direct participation in the reaction. After HBr is consumed and the ratio is <1:4000, the HOCl + HCl reactions become predominant.

Acknowledgment. This study was supported by the Austrian Science Fund (project number P14357-TPH). C.T. is grateful for financial support by the University of Innsbruck. T.L. is grateful to the Austrian Academy of Sciences for financial support.

Supporting Information Available: Geometrical details and a comparison with previous studies. This material is available free of charge via the Internet at http://pubs.acs.org.

References and Notes

(1) Molina, M. J.; Rowland, F. S. *Nature (London)* **1974**, *249*, 810−812.
(2) Farman, J. G.; Gardiner, B. G.; Shanklin, J. D. *Nature (London)* **1985**, *315*, 207−210.
(3) McElroy, M. B.; Salawitch, R. J.; Wofsy, S. C.; Logan, J. A. *Nature (London)* **1986**, *321*, 759−762.
(4) Solomon, S.; Garcia, R. R.; Rowland, F. S.; Wuebbles, D. J. *Nature (London)* **1986**, *321*, 755−758.
(5) Finlayson-Pitts, B. J.; Pitts, J. N., Jr. *Chemistry of the Upper and Lower Atmosphere*; Academic Press: San Diego, CA, 2000.
(6) Solomon, S. *Rev. Geophys.* **1999**, *37*, 275−316.
(7) Prather, M. J. *Nature (London)* **1992**, *255*, 534−537.
(8) Chu, L.; Chu, L. T. *J. Phys. Chem. A* **1999**, *103*, 691−699.
(9) Crutzen, P. J.; Müller, R.; Brühl, C.; Peter, T. *Geophys. Res. Lett.* **1992**, *19*, 1113−1116.
(10) Hanson, D. R.; Lovejoy, E. R. *J. Phys. Chem.* **1996**, *100*, 6397−6405.
(11) Abbatt, J. P. D.; Nowak, J. B. *J. Phys. Chem. A* **1997**, *101*, 2131−2137.
(12) Richardson, S. L.; Francisco, J. S.; Mebel, A. M.; Morokuma, K. *Chem. Phys. Lett.* **1997**, *270*, 395−398.
(13) Liu, Z. F.; Siu, C. K.; Tse, J. S. *Chem. Phys. Lett.* **1999**, *309*, 335−343.
(14) Xu, S. C. *J. Chem. Phys.* **1999**, *111*, 2242−2254.
(15) Zhou, Y.-F.; Liu, C.-B. *Int. J. Quantum Chem.* **2000**, *78*, 281−284.
(16) Kroes, G.-J.; Clary, D. C. *J. Phys. Chem.* **1992**, *96*, 7079−7088.
(17) Packer, M. J.; Clary, D. C. *J. Phys. Chem.* **1995**, *99*, 14323−14333.
(18) Wang, L.; Clary, D. C. *J. Chem. Phys.* **1996**, *104*, 5663−5673.
(19) Re, S.; Osamura, Y.; Suzuki, Y.; Schaefer, H. F., III. *J. Chem. Phys.* **1998**, *109*, 973−977.
(20) Bussolin, G.; Casassa, S.; Pisani, C.; Ugliengo, P. *J. Chem. Phys.* **1998**, *108*, 9516−9528.
(21) Geiger, F. M.; Hicks, J. M.; de Dios, A. C. *J. Phys. Chem. A* **1998**, *102*, 1514−1522.
(22) Dibble, T. S.; Francisco, J. S. *J. Phys. Chem.* **1995**, *99*, 1919−1922.
(23) Brown, A. R.; Doren, D. J. *J. Phys. Chem. A* **1997**, *101*, 6308−6312.
(24) Zhou, Y. F.; Liu, C. B. *J. Phys. Chem. Solids* **1999**, *60*, 2001−2004.
(25) Stephens, P. J.; Devlin, F. J.; Chabalowski, C. F.; Frisch, M. J. *J. Phys. Chem.* **1994**, *98*, 11623−11627.
(26) Lynch, B. J.; Fast, P. L.; Harris, M.; Truhlar, D. G. *J. Phys. Chem. A* **2000**, *104*, 4811−4815.
(27) Peng, C.; Ayala, P. Y.; Schlegel, H. B. *J. Comput. Chem.* **1996**, *17*, 49−56.
(28) Durant, J. L. *Chem. Phys. Lett.* **1996**, *256*, 598−602.
(29) Jursic, B. S. *THEOCHEM (J. Mol. Struct.)* **1997**, *417*, 89−94.
(30) Lynch, B. J.; Truhlar, D. G. *J. Phys. Chem. A* **2001**, *105*, 2936−2941.

(31) Becke, A. D. *J. Chem. Phys.* **1993**, *98*, 5648−5652.
(32) Adamo, C.; Barone, V. *Chem. Phys. Lett.* **1997**, *274*, 242−250.
(33) Adamo, C.; Barone, V. *J. Chem. Phys.* **1998**, *108*, 664−675.
(34) Lynch, B. J.; Truhlar, D. G. *J. Phys. Chem. A* **2002**, *106*, 842−846.
(35) Curtiss, L. A.; Raghavachari, K.; Trucks, G. W.; Pople, J. A. *J. Chem. Phys.* **1991**, *94*, 7221−7230.
(36) Curtiss, L. A.; Raghavachari, K.; Pople, J. A. *J. Chem. Phys.* **1993**, *98*, 1293−1298.
(37) Curtiss, L. A.; Raghavachari, K.; Redfern, P. C.; Pople, J. A. *J. Chem. Phys.* **1998**, *109*, 7764−7776.
(38) Curtiss, L. A.; Redfern, P. C.; Raghavachari, K.; Rassolov, V.; Pople, J. A. *J. Chem. Phys.* **1999**, *110*, 4703−4709.
(39) Raghavachari, K.; Trucks, G. W.; Pople, J. A.; Head-Gordon, M. *Chem. Phys. Lett.* **1989**, *157*, 479−483.
(40) Møller, C.; Plesset, M. S. *Phys. Rev.* **1934**, *46*, 618−622.
(41) Dunning, T. H., Jr. *J. Chem. Phys.* **1989**, *90*, 1007−1023.
(42) Lee, T. J.; Taylor, P. R. *Int. J. Quantum Chem., Quantum Chem. Symp.* **1989**, *23*, 199−207.
(43) Page, M.; McIver, J. W., Jr. *J. Chem. Phys.* **1988**, *88*, 922−935.
(44) Chuang, Y.-Y.; Truhlar, D. G. *J. Phys. Chem. A* **1997**, *101*, 3808−3814.
(45) Eyring, H. *J. Chem. Phys.* **1935**, *3*, 107−115.
(46) Corchado, J. C.; Chuang, Y.-Y.; Fast, P. L.; Villá, J.; Hu, W.-P.; Liu, Y.-P.; Lynch, G. C.; Nguyen, K. A.; Jackels, C. F.; Melissas, V. S.; Lynch, B. J.; Rossi, I.; Coitiño, E. L.; Fernandez-Ramos, A.; Steckler, R.; Garrett, B. C.; Isaacson, A. D.; Truhlar, D. G. *Polyrate*, version 8.5.1; University of Minnesota: Minneapolis, MN, 2000.
(47) Corchado, J. C.; Chuang, Y.-Y.; Coitiño, E. L.; Truhlar, D. G. *Gaussrate*, version 8.6; University of Minnesota: Minneapolis, MN, 2000.
(48) Truhlar, D. G.; Hase, W. L.; Hynes, J. T. *J. Phys. Chem.* **1983**, *87*, 2664−2682.
(49) Truhlar, D. G.; Garrett, B. C. *Annu. Rev. Phys. Chem.* **1984**, *35*, 159−189.
(50) Truhlar, D. G.; Isaacson, A. D.; Garrett, B. C. In *Theory of Chemical Reaction Dynamics*; Baer, M., Ed.; CRC Press: Boca Raton, FL, 1985; Chapter 2, pp 65−137.
(51) Kreevoy, M. M.; Truhlar, D. G. In *Investigation of Rates and Mechanisms of Reactions*; Bernasconi, C. F., Ed.; John Wiley & Sons: New York, 1986; Chapter 1, pp 13−95.
(52) Tucker, S. C.; Truhlar, D. G. In *New Theoretical Concepts for Understanding Organic Reactions*; Bertrán, J., Csizmadia, I. G., Eds.; NATO ASI Series C 267; Kluwer: Dordrecht, The Netherlands, 1989; pp 291−346.
(53) Truhlar, D. G. In *The Reaction Path in Chemistry: Current Approaches and Perspectives*; Heidrich, D., Ed.; Kluwer: Dordrecht, The Netherlands, 1995; pp 229−255.
(54) Truhlar, D. G.; Garrett, B. C.; Klippenstein, S. J. *J. Phys. Chem.* **1996**, *100*, 12771−12800.
(55) Wigner, E. *Z. Phys. Chem., Abt. B* **1932**, *32*, 203−216.
(56) Marcus, R. A.; Coltrin, M. E. *J. Chem. Phys.* **1977**, *67*, 2609.
(57) Skodje, R. T.; Truhlar, D. G.; Garrett, B. C. *J. Phys. Chem.* **1981**, *85*, 3019−3023.
(58) Baldridge, K. K.; Gordon, M. S.; Steckler, R.; Truhlar, D. G. *J. Phys. Chem.* **1989**, *93*, 5107−5119.
(59) Fernández-Ramos, A.; Truhlar, D. G. *J. Chem. Phys.* **2001**, *114*, 1491−1496.
(60) Oliphant, N.; Bartlett, R. J. *J. Chem. Phys.* **1994**, *100*, 6550−6561.
(61) Jensen, F. *Introduction to Computational Chemistry*; Wiley & Sons: New York, 1999.
(62) Uras-Aytemiz, N.; Joyce, C.; Devlin, J. P. *J. Phys. Chem. A* **2001**, *105*, 10497−10500.
(63) Xu, S. C.; Zhao, X. S. *J. Phys. Chem. A* **1999**, *103*, 2100−2106.
(64) Loerting, T.; Liedl, K. R.; Rode, B. M. *J. Am. Chem. Soc.* **1998**, *120*, 404−412.
(65) Loerting, T.; Liedl, K. R.; Rode, B. M. *J. Chem. Phys.* **1998**, *109*, 2672−2679.
(66) Loerting, T.; Liedl, K. R. *Chem.—Eur. J.* **2001**, *7*, 1662−1669.
(67) Tautermann, C. S.; Voegele, A. F.; Loerting, T.; Kohl, I.; Hallbrucker, A.; Mayer, E.; Liedl, K. R. *Chem.—Eur. J.* **2002**, *8*, 66−73.